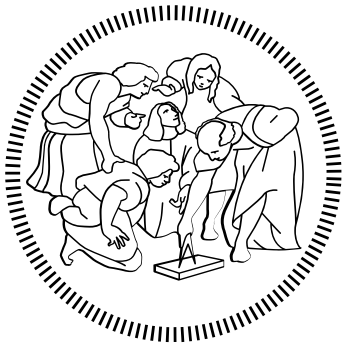

POLITECNICO
MILANO 1863

Modeling of a blow-down propulsion system

Course of Space Propulsion
Academic Year 2023-2024

Lockheed Martini Group

Alessandro Pallotta	alessandro1.pallotta@mail.polimi.it	10712370
Alex Cristian Turcu	alexcristian.turcu@mail.polimi.it	10711624
Chiara Poli	chiara3.poli@mail.polimi.it	10731504
Daniele Paternoster	daniele.paternoster@mail.polimi.it	10836125
Marcello Pareschi	marcello.pareschi@mail.polimi.it	10723712
Paolo Vanelli	paolo.vanelli@mail.polimi.it	10730510
Riccardo Vidari	riccardo.vidari@mail.polimi.it	10711828

Contents

Nomenclature

Acronyms

AM	Additive Manufacturing
DRY-1	Engine Name
LRE	Liquid Rocket Engine
LOX	Liquid Oxygen
RP-1	RP-1 fuel

Symbols

a	[m/s]	Speed of sound
A	[m^2]	Area
B	[-]	Blow-down ratio
c	[J/kg K]	Specific heat
c_P	[J/kg K]	Specific heat at constant pressure
c_T	[-]	Thrust coefficient
c^*	[m/s]	Characteristic velocity
C_d	[-]	Discharge coefficient
D	[m]	Diameter
E	[m/s]	Erosion rate
f	[-]	Darcy friction factor
h_g	[W/m^2 K]	Gas-side convective heat transfer coefficient
H	[m]	Height
i	[-]	First iteration index
I_{sp}	[s]	Specific impulse
I_{tot}	[N s]	Total impulse
j	[-]	Second iteration index
k	[m^{-1}]	Curvature
K	[-]	Pressure loss coefficient
L	[m]	Length
L^*	[m]	Characteristic length
m	[kg]	Mass
$\dot{m}$	[m/s]	Mass flow rate
M	[-]	Mach number
$\mathbb{M}$	[kg/mol]	Molar mass
N	[-]	Number of
O/F	[-]	Oxidizer to fuel ratio
$\overline{O/F}$	[-]	Mean O/F ratio
p	[Pa]	Pressure
Δp	[Pa]	Pressure loss / difference
Pr	[-]	Prandtl number
$\dot{q}$	[W/m^2]	Heat flux
$\dot{Q}$	[W]	Heat transfer rate
r	[-]	Recovery factor
R	[J/kg K]	Specific gas constant
$\mathcal{R}$	[J/mol K]	Universal gas constant
Re	[-]	Reynolds number
Re'	[-]	Modified Reynolds number
t	[s]	Time
Δt	[s]	Time step
T	[K]	Temperature
ΔT	[K]	Variation of temperature
$\mathbb{T}$	[N]	Thrust
u	[m/s]	Velocity
V	[m^3]	Volume
ΔV	[m^3]	Volume change
α_{AM}	[deg]	Deposition angle of AM
α_{con}	[deg]	Convergent semi-aperture angle
β	[%]	Injector pressure drop as percentage of initial combustion chamber pressure
γ	[-]	Heat capacity ratio
ε	[-]	Area ratio
λ	[-]	Nozzle losses coefficient
μ	[Pa s]	Dynamic viscosity
ρ	[kg/m^3]	Density
σ	[-]	Correction factor across boundary layer

Subscripts

aw	Adiabatic wall	**inj**	Injector
c	Combustion chamber	**max**	Maximum
cea	From CEAM software	**min**	Minimum
co	Coolant	**ox**	Oxidizer
con	Convergent	**p**	Propellants
e	Nozzle exit	**pr**	Pressurizer gas
eff	Effective	**r**	Real
f	Final	**t**	Nozzle throat
fd	Feeding lines	**tc**	Thrust chamber
fu	Fuel	**tk**	Tank
i	Initial	**tot**	Total
id	Ideal	**wg**	Gas side wall

1 Introduction and literature overview

In this work a preliminary design of a 1 kN semi-cryogenic LRE (LOX/RP-1) equipped with a blow-down feeding system is discussed. In particular, a first literature analysis was done in order to review previous studies regarding this particular architecture. Recent developments in additive manufacture (AM) techniques were analyzed to obtain some knowledge regarding processes and precision of this new frontier. Moreover, due the reduced size of this system, some criticalities regarding boundary layer and erosion losses were researched. The second part of the paper aim at designing the engine with some imposed initial conditions and some assumptions. The whole dimensioning of the system, including the tanks and feeding lines, is carried on including the dynamics of the system. The final sizing will accomplish the maximization of the total impulse, with the initial and final constraints. An off-design analysis is then performed to quantify the performances with nozzle losses and AM uncertainties. Finally, a feasibility analysis of nozzle fuel cooling is discussed.

1.1 Blow-down heritage

The blow-down architecture is the simplest feeding technique for LRE since it does not require additional pressurizing gas tanks with failure-prone pressure regulator valves nor complex turbomachinery. The scheme includes only two liquid propellant tanks filled with helium or nitrogen, eventually separated by a membrane. The major downsides of this simplicity is relative to the non-stationarity of the tank pressures that induce chamber pressure drop, decrease of propellant mass flow rate and as a consequence O/F ratio variation. This chain of events degrades performances overtime and must be carefully evaluated since combustion efficiency relies upon viable domains of injection pressure and correct mass flow ratio. The interest on blow-down is although justified with respect to well-known pressure regulated feed system since this last can also manifest some criticalities in terms of long-term reliability. In particular, propulsion systems play crucial roles for mission success, such as long interplanetary trips, and they must ensure failure-free lifetime. This is a major concern when focusing on pressure regulated feeding lines in which a pressure regulator valve is present. This kind of elements can be quite complex and hence add a weakness for the whole system[1]. Considering these facts, a blow-down type architecture could be of interest since it decrease system complexity. Moreover, different feasibility analysis for blow-down units are present in the literature in which also an external re-pressurization tank is considered[2]. This is an upgrade that allows to recover performance of the feeding pressure and hence combustion properties. Although the valve complexity is removed since a pyro valve can be used to discharge the gas with a single shot application, the eventual re-pressurization can be a crucial point as the sudden change in pressure could induce unwanted instabilities. Other configurations could foresee the use of a Venturi valve to maintain constant mass flow rate by cavitating the liquid and choking the flow on the feeding line. However, neither extra tank nor Venturi valves will be considered in this work in order to meet the requirements presented in **REFERENCE** .
The whole evaluation of the dynamics of the examined propulsion system was not based upon previous works, instead a self-made model was developed.

1.2 Additive manufacturing state of art

1.3 Analysis of losses

2 Modelling of propulsion system: DRY-1

The workflow for the sizing of DRY-1 is introduced by Figure 1 and it is divided into three stages:

- **Input data**: the problem is set up.
- **Nominal sizing**: the system is sized according to initial conditions and general assumptions.
- **System dynamics**: an iterative process is set up to model the blow-down dynamics and finalize the sizing.

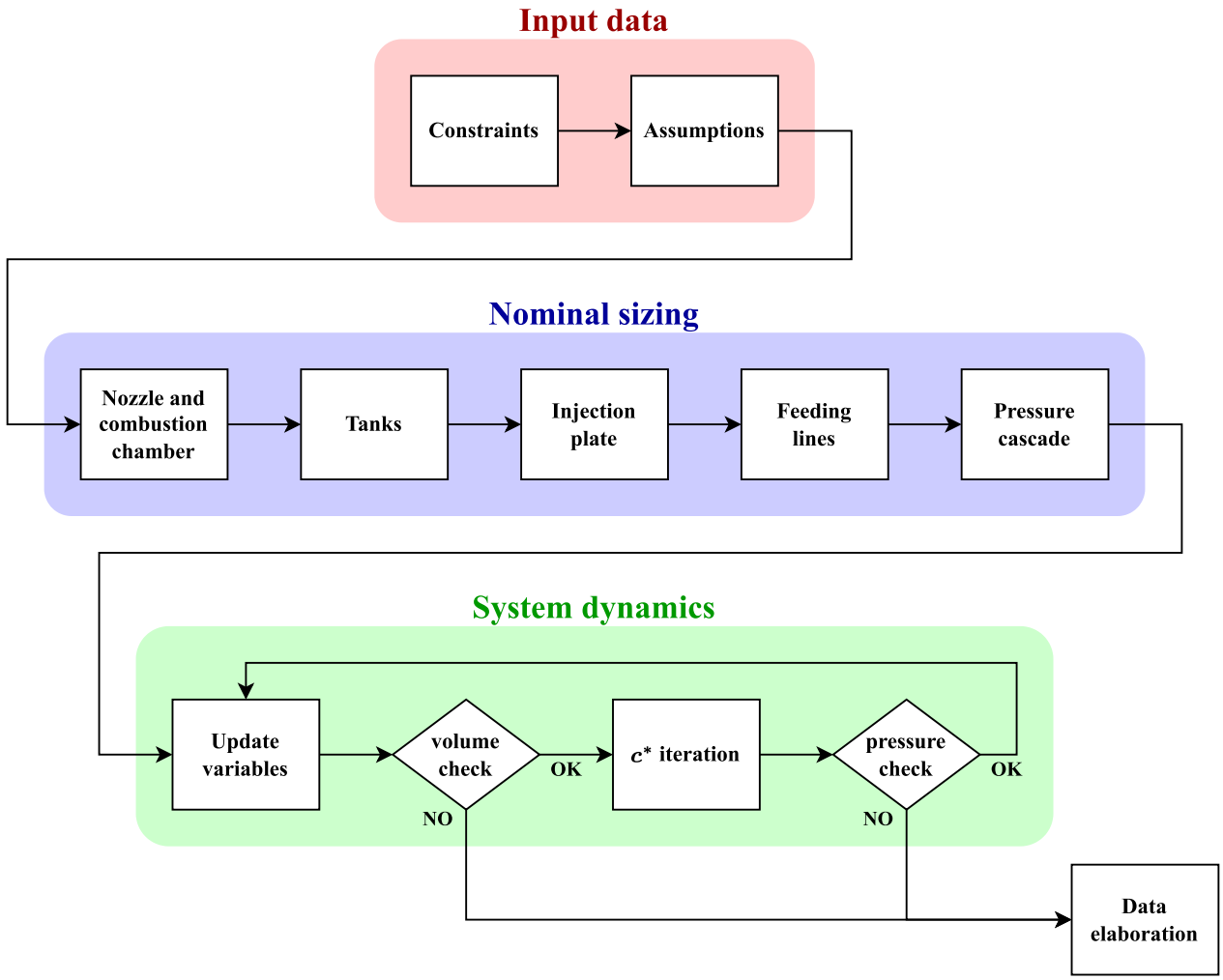

Figure 1: Flowchart of the simulation model

2.1 Input data

The input data defined different kind of requirements, related to operability environment, engine performance, size constraints, chemistry, architecture and manufacturing techniques. Regardless of the development of the engine design, the system shall respect the following pinpoints:

- **Environment**: vacuum for the whole operation.
- **Thrust** $\mathbb{T}$: initial magnitude of 1 kN, no lower boundary.
- **Chamber pressure** p_c: initial value of 50 bar, always above 20 bar throughout the whole mission.
- **Allocated space**: tanks, combustion chamber and convergent nozzle occupancy is exactly 80% of the volume occupied by a cylinder of 1 meter diameter and 2 meter length. No bounds on the extension of the divergent.
- **Propellants**: semi-cryogenic couple of LOX and RP-1.
- **Architecture**: blow-down type.
- **Manufacturing**: all the system is produced in AM, no restriction on material nor techniques.

The nominal sizing refers to the design of the overall system considering the imposed initial constraints as static conditions. This design choice was dictated by the dynamics of the blow-down system, which imposes the maximum flow rate at the beginning of the mission, leading to the oversizing of the engine throughout the rest of the mission.
Various hypothesis were necessary to develop the system, this values are reported in Table 1.

O/F [-]	ε [-]	ε_{con} [-]	L^* [m]
2.42	300	10	1.143

Table 1: Hypothesis from literature and previous design

The choices of L^* and O/F were only dictated by the propellant couple[3], while ε was chosen as the characteristic of the engine refers to an in-space application[4]. Regarding the value of ε_{con} a mean value between 5 and 15 was taken. Smaller values entails longer combustion chamber and small cross sectional area, with large pressure drops. Larger values refers to bigger chamber cross sectional area, with limited length for the combustion. From the literature the suggestion for the choice of this value is to refer to previous successful engines design, considering the same application[5]. Therefore, a 400 N bi-propellant apogee motor was taken as reference and revealed a value of $\varepsilon_{con} \approx 10$[4].

2.2 Nominal sizing

After defining the main input data, the workflow is carried out as shown in Figure 1. All the combustion simulations were performed with Nasa-CEA software, implemented in Matlab (CEAM). In particular the "rocket problem" was considered, Bray model was applied for the expansion (frozen point at the throat), infinite combustion chamber ($M_c = 0$), initial injecting temperatures of the propellant equal to the storage temperatures. The chamber pressure was set as $p_c = 50$ bar and the mixture ratio as $O/F = 2.42$. Latter refinement of this last value will be performed. The output values used from the simulation are represented (vacuum value is considered for the c_T):

c^* [m/s]	c_T [-]	T_c [K]	γ_c [-]
1851	1.935	3708	1.1405

Table 2: First run on CEAM

From this results, the propellant mass flow rate and the throat area can be calculated:

$$\dot{m}_p = \frac{\mathbb{T}}{c_T c^*} \qquad A_t = \frac{\dot{m}_p c^*}{P_c} \tag{1}$$

From the geometry assumption of Table 1, the nozzle exit area and the combustion chamber geometry can be retrieved:

$$A_e = \varepsilon A_t \tag{2}$$

$$A_c = \varepsilon_{con} A_t \qquad L_c = \frac{L^*}{\varepsilon_{con}} \tag{3}$$

Nozzle geometry model will be delved in section 4. The results for the previous calculation are the following:

$\dot{m}_p$ [kg/s]	D_t [cm]	D_e [cm]	D_c [cm]	L_c [cm]
0.279	1.15	19.86	3.63	11.43

Table 3: Preliminary DRY-1 geometry

A check on the compliance of the chamber Mach number is done ($M_c < 0.3$):

$$\frac{1}{\varepsilon_{con}} = M_c \left[\frac{1 + \frac{\gamma_c - 1}{2}}{1 + \frac{\gamma_c - 1}{2} M_c^2} \right]^{\frac{\gamma_c + 1}{2(\gamma_c - 1)}} \xrightarrow{fsolve} \qquad M_c = 0.059 \tag{4}$$

From the geometry of the motor and the allocated space constraints, the total height of the tanks can be calculated. The volume around the thrust chamber (combustion chamber + convergent) can be assessed:

$$V_{tc} = \frac{\pi}{4}\left[L_c D_c^2 + \frac{L_{con}}{3}\left(D_c^2 + D_t^2 + D_c D_t\right)\right] \tag{5}$$

Also, the volume of the cylinder that covers the length of the thrust chamber and with the total diameter of 1 meter (D_{tot}) can be computed. From there, the empty volume around the thrust chamber can be computed as a difference:

$$V_{lost} = V_{tc} - \frac{\pi}{4}\left(L_c + L_{con}\right) D_{tot} \tag{6}$$

This value must be 20% of the total cylinder volume, as cited in subsection 2.1. As the computed value was lower, additional volume had to be removed from the tanks in order to meet the requirement. The height dedicated to the tanks is calculated as follow:

$$H_{tk} = H - \left[L_c + L_{con} + \frac{4}{\pi D_{tot}^2}\left(0.2 V_{tot} - V_{lost}\right)\right] \tag{7}$$

The total volume allocated to the tanks is hence fully defined. In order to calculate the masses of pressurizer and propellants, some assumption have to be made:

- adiabatic expansion of the pressurizing gas;
- blow-down ratios can be tuned;
- mean value of the oxidizer to fuel ratio.

A system of equations can be set up:

$$\begin{cases} \dfrac{m_{ox}}{m_{fu}} = \overline{O/F} \\ m_{ox} = \rho_{ox} V_{ox} \\ m_{fu} = \rho_{fu} V_{fu} \\ V_{ox} = V_{pr,f}^{ox} - V_{pr,i}^{ox} \\ V_{fu} = V_{pr,f}^{fu} - V_{pr,i}^{fu} \\ V_{pr,f}^{ox} = B_{ox}^{\frac{1}{\gamma_{pr,ox}}} V_{pr,i}^{ox} \\ V_{pr,f}^{fu} = B_{fu}^{\frac{1}{\gamma_{pr,fu}}} V_{pr,i}^{fu} \end{cases} \tag{8}$$

In order to solve System 8, the pressurizer and the initial temperature of the propellants have to be set. Different pressurizing gas are available, mainly nitrogen or helium are the most common choices. The main differences for the two are the storage temperature, the molar mass and the specific heat ratio. The latter parameter influences the adiabatic discharge, higher values implies faster pressure discharge. The molar mass affects the amount of gas to be embarked at a given pressure. The storage temperature is a matter of compatibility with the propellant. Nitrogen gas was chosen to pressurize RP-1 since no cryogenic conditions were present also it guarantees lower discharge, with the downside of increasing the mass of the system. On the other side, LOX required a cryogenic compatibility that can be ensured by helium. Even though an efficient insulating bladder is employed, the design choice was dictated by a more conservative approach: the employment of nitrogen also with LOX was discarded since storage temperature and pressure are not compatible with its properties[6].

$T_{pr,fu}$ [K]	$T_{pr,ox}$ [K]	γ_{N_2} [-]	γ_{He} [-]
300	90	1.40	1.67

Table 4: Initial values for pressurizer gases and specific heat ratio values

$\overline{O/F}$ [-]	$B_{pr,ox}$ [-]	$B_{pr,fu}$ [-]	V_{tot} [m^3]
2.42	2.5	2.5	1.27

Table 5: Assumed or calculated values as first iteration

HO INSERITO I DATI, DOBBIAMO COMMENTARLI
The masses and volumes of oxidizer, fuel and pressurizing gases are computed.

m_{fu} [kg]	m_{ox} [kg]	$V^{fu}_{pr,i}$ [m^3]	$V_{fu,i}$ [m^3]	$V^{ox}_{pr,i}$ [m^3]	$V_{ox,i}$ [m^3]
165.34	400.13	0.2217	0.2049	0.4789	0.3510

Table 6: Propellant and pressurizer quantities as first iteration

HO INSERITO I VALORI TROVATI DALLA PRIMA ITERAZIONE
Finally, the feeding lines can be modelled. Considering figure **REFERENCE** , the length of the pipes can be retrieved as a difference:

$$L_{fd,fu} = H - L_c - H_{tk,fu} \tag{9}$$

$$L_{fd,ox} = H - L_c - H_{tk} \tag{10}$$

To completely determine the DRY-1 geometry, the injection plate must be modelled. The pressure drop across the injector Δp_{inj} have to be assumed as a percentage of the initial chamber pressure. Acceptable range of this fraction goes from 5% to 30%. A value of 20% is chosen for both oxidizer and fuel lines. The fuel and oxidizer injector area can be computed assuming reasonable values for the discharge coefficient C_d. A reasonable assumption has been made according to the superficial roughness quality of AM.

$$\dot{m}_{fu} = \frac{1}{1+O/F}\dot{m}_p \qquad \dot{m}_{ox} = \frac{O/F}{1+O/F}\dot{m}_p \tag{11}$$

$$A_{inj,tot} = \frac{\dot{m}_p}{C_d\sqrt{2\Delta p_{inj}\rho_p}} \tag{12}$$

$$K_p = 1 + f\frac{L_{p,fd}}{D_{p,fd}}\left(\frac{A_{p,fd}}{A_{p,inj,tot}C_d}\right)^2 \tag{13}$$

PERDITE DI CARICO GENERALIZZATE

2.3 System dynamics

From the nominal sizing of the engine, it is necessary to simulate the real dynamics of the system in order to:

- retrieve the performance of the designed system in time;
- check the compliance of the system with the constraints;
- test other designs through iteration to select the best one based on the simulated data of interest.

For this reasons, a numerical method was implemented. An high level explanation for the functioning of the algorithm can be appreciated in Figure 2.

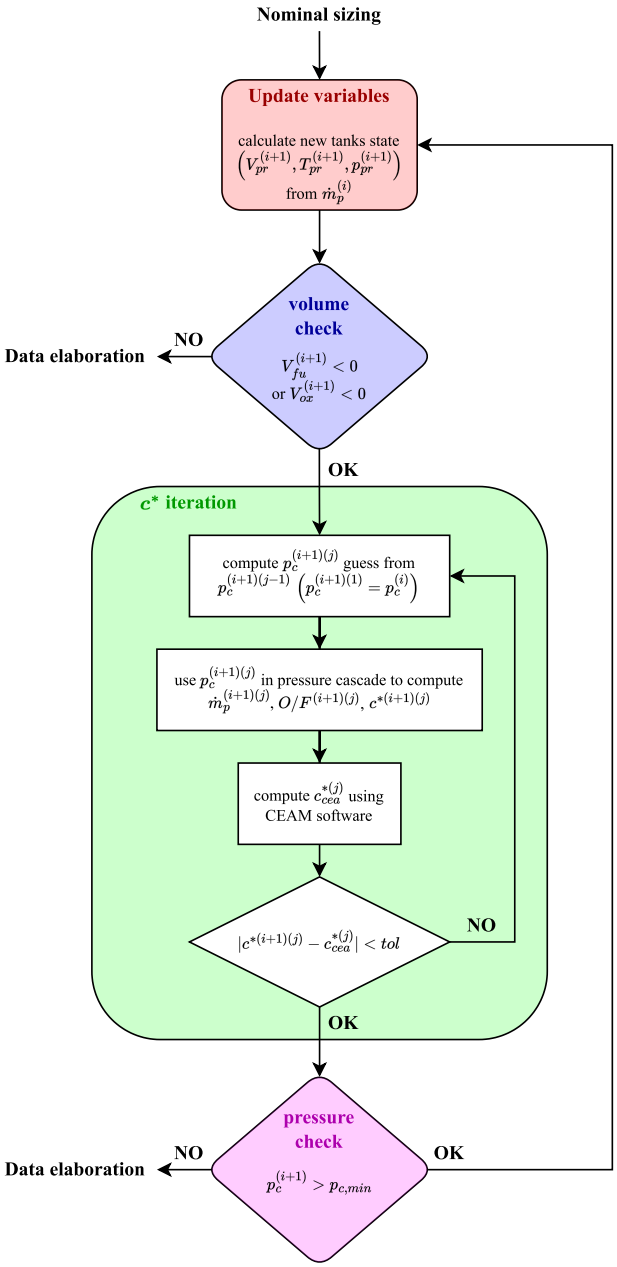

Figure 2: Flowchart of dynamics of the model

The first step of the time cycle is to update the state of the two tanks based on the previous iteration. Assuming a constant propellants flow rate during the time step Δt, the volume of the remaining liquid is decreased by a quantity $\Delta V^{(i+1)}$. Accordingly, the volume of the pressurizer will increase by the same amount.

$$\Delta V^{(i+1)} = \frac{\dot{m}_p^{(i)} \Delta t}{\rho_p} \tag{14}$$

$$V_p^{(i+1)} = V_p^{(i)} - \Delta V^{(i+1)} \tag{15}$$

$$V_{pr}^{(i+1)} = V_{pr}^{(i)} + \Delta V^{(i+1)} \tag{16}$$

From the change of volume, the new pressure and temperature of the pressurizer gas are computed assuming

an adiabatic expansion in the tank:

$$p_{pr}^{(i+1)} = p_{pr}^{(i)} \left(\frac{V_{pr}^{(i)}}{V_{pr}^{(i+1)}} \right)^{\gamma_{pr}} \tag{17}$$

$$T_{pr}^{(i+1)} = T_{pr}^{(i)} \left(\frac{V_{pr}^{(i)}}{V_{pr}^{(i+1)}} \right)^{\gamma_{pr}-1} \tag{18}$$

A check must be performed on the remaining volume of propellants in the tanks at current iteration: if the volume of fuel is negative it means that the combustion is over so the simulation stops (the same for oxidizer). If there is some more propellant to use, the iteration goes on with the calculation of the new chamber pressure. This step is complex because it introduces another cycle of iterations inside each time step. The mass flow rate of the propellants depends on the pressure cascade in the feeding lines, hence on the chamber pressure. These two variables are bounded and both unknown, but there's only one configuration that can match the boundary condition imposed by the critical condition in the throat, so the problem is well-posed.
From literature, the c^* of the chamber has the following expression:

$$c^* = \frac{p_c A_t}{\dot{m}_{fu} + \dot{m}_{ox}} \tag{19}$$

It correlates the chamber pressure with the propellants flow rate in the throat. Moreover, it only depends on the thermodynamics of the combustion process in the chamber, which changes over time due to the architecture of blow-down system. By imposing the critical conditions in the throat, it can be rewritten as:

$$c^* = \sqrt{\frac{\mathcal{R}}{\mathbb{M}} \frac{T_c}{\gamma} \left(\frac{\gamma+1}{2} \right)^{\frac{\gamma+1}{\gamma-1}}} \tag{20}$$

The system is coherent only if the two expressions give the same result. A system of equations could be created and numerically solved to match both the pressure cascade and c^*.
A reasonable initial guess for chamber pressure $p_c^{(i+1)(1)}$ is taken as the pressure at previous time step $p_c^{(i)}$. The next steps $p_c^{(i+1)(j)}$ will converge progressively towards the real current pressure $p_c^{(i+1)}$ (for increasing j).
From $p_c^{(i+1)(j)}$ the $c^{*(i+1)(j)}$ is computed from the pressure cascade as described in Equation 19:

$$u_{fd,p}^{(i+1)(j)} = \sqrt{\frac{2\left(p_{pr}^{(i+1)} - p_c^{(i+1)(j)}\right)}{\rho_p K_p}} \tag{21}$$

$$m_p^{(i+1)(j)} = \rho_p A_{fd,p} u_{fd,p}^{(i+1)(j)} \tag{22}$$

$$O/F^{(i+1)(j)} = \frac{m_{ox}^{(i+1)(j)}}{m_{fu}^{(i+1)(j)}} \tag{23}$$

$$c^{*(i+1)(j)} = \frac{A_t p_c^{(i+1)(j)}}{\dot{m}_{fu}^{(i+1)(j)} + \dot{m}_{ox}^{(i+1)(j)}} \tag{24}$$

Equation 20 is solved directly using CEAM software, which takes as input $p_c^{(i+1)(j)}$ and $O/F^{(i+1)(j)}$ to return $c_{cea}^{*(j)}$.
The two computed c^* are then compared: if their difference satisfies a certain tolerance, then the cycle stops and returns the new values for the current time step. Else, the inner cycle continues the refinement by guessing a new $p_c^{(i+1)(j+1)}$ from $p_c^{(i+1)(j)}$.
Finally, a check on the new combustion pressure $p_c^{(i+1)}$ is performed in order to stay above the minimum design pressure $p_{c,min}$, as mentioned in **REFERENCE** . Similarly to the previous check, if the pressure drops below the limit the simulation stops and returns the results, else it continues with the next time step.

The same general algorithm is used to refine the initial assumptions of O/F and B, which influence the nominal design of the whole engine (as described in subsection 2.2). In this case, the initial c^* value from design

is assumed constant to reduce the computational burden, since the algorithm is applied over a wide range of combinations of O/F and B. This assumption is reasonable because the O/F (and as consequence the thermodynamics of the combustion) hardly varies during the whole burn, as can be noticed in **REFERENCE** .

3 Results analysis

4 Nozzle losses

5 Additive manufacturing influences

6 Cooling analysis

In this section a preliminary feasibility analysis for cooling of the DRY-1 engine with RP-1 is discussed. High temperatures reached in the combustion chamber and nozzle have to deeply discussed at this first stage of the design since it could have deep consequences on the architecture, materials choice and performances of the engine. The following analysis is necessary to evaluate the researched feasibility of RP-1 as a coolant. In this context, it is possible to make reference to past successful engine design since kerosene cooling has been of fundamental importance for vast applications.
Two kinds of techniques could be considered with this propellant, regenerative cooling and film cooling. The last one is used along the lateral surface of the combustion chamber to create a fuel layer that protects the chamber, with a slight decrease on the performance. This strategy has demonstrated great effectiveness for in-space and low pressure engines[7], an example of this is given by the previously cited 400-N Liquid Rocket engine for in-space applications[4]. DRY-1 could exploit film cooling as a viable option thats is also enhanced by previous successful design for this small-thrust kind of motor. Clearly, the feasibility shall be quantitatively assessed.
On the other way, regenerative cooling techniques are not frequently seen on small thrust or low pressure chamber pressure applications since the critical point of the process relies on having sufficient pressure for the fuel line that is affected by losses along the cooling jacket. Considering the DRY-1 blow-down architecture, the critical points would be:

- **Fuel feeding line pressure losses**: the pressure in the lines of feeding is varying along the operation, in particular at the end of the mission low fuel pressure could not match the requirement of pressure at the combustion chamber.
- **Variation of boiling temperature**: due to variation of fuel feeding pressure, also the vaporization temperature varies. In general temperature shall be assessed through the pipes to evaluate if decomposition or vaporization of RP-1 is happening.

6.1 Mathematical model for the gas heat transfer

The workflow of this section is to evaluate whether the total heat flux generated by the gas flow (as convective heat) can be absorbed by the coolant without exceeding temperature constraint of the RP-1. Different approaches and assumptions can be made to breakdown the problem. In this case it is assumed to have a one-dimensional flow (perpendicular to the expanded gas flow), the heat is exchanged only by forced convective processes (disregarding the radiation coming from the flow), steady state assumption is made. Some other assumptions will be presented during the following development. Regarding the model of convective heat transfer from the hot gases to the wall, it can be mathematically described as:

$$\dot{q} = h_g(T_{aw} - T_{wg}) \tag{25}$$

The temperature considered for the gas flow T_{aw} is referred as the total adiabatic wall temperature and is calculated as:

$$T_{aw} = T_c \left[\frac{1 + r\left(\frac{\gamma-1}{2}\right) M^2}{1 + \left(\frac{\gamma-1}{2}\right) M^2} \right] \qquad r = Pr^{0.33} \tag{26}$$

Where Mach number is the one relative to the axial distance, in which T_{wg} has to be calculated, the recovery

factor r depends on the local Prandtl number. Also γ is assessed at axial coordinate of interest. T_{wg} is the static temperature of the wall on the internal side. T_{aw} is the temperature driving the heat transfer and it is slightly less then stagnation temperature of the gas due to the back heat effect generated by the compressible and viscous boundary layer near the chamber wall. The difficulty relies on establishing the value of the convective heat transfer h_g, different empirical models are present in the literature. One of the most used and commonly applied is the Bartz relation given as:

$$h_g = \left(\frac{0.026}{D_t^2}\right)\left(\frac{\mu^{0.2} c_P}{Pr^{0.6}}\right)_c \left(\frac{p_c}{c^*}\right)^{0.8} \left(\frac{D_t}{k_t}\right)^{0.1} \left(\frac{A_t}{A}\right)^{0.9} \sigma \tag{27}$$

$$\sigma = \frac{1}{\left[\frac{1}{2}\frac{T_{wg}}{T_c}\left(1 + \frac{\gamma+1}{2}M^2 + \frac{1}{2}\right)\right]^{0.68} \left[1 + \frac{\gamma-1}{2}M^2\right]^{0.12}} \tag{28}$$

Regarding Equation 27, it depends on the geometry of the nozzle and chamber conditions. The area ratio of the same formula gives the dependence on the axial distance. The factor σ in Equation 28 is also dependent on the axial distance of the nozzle since it contains the Mach number and the temperature of the wall on the gas side at that location. In the same equation, γ is also referred to the local value at that position. It can be noticed that the unknown temperature T_{wg} is present also in the h_g coefficient: an assumption on the wall temperature must be taken. In particular, when the material of the nozzle wall is defined, also a maximum allowed temperature is provided. A reasonable assumption for the adiabatic temperature distribution T_{wg} can be done assuming that the ratio $T_{wg}(x)/T_{aw}(x)$ is constant and equal at the same ratio evaluated at the nozzle inlet, imposing $T_{wg} = T_{max}$ at the nozzle entrance. In Figure 3 it is represented the distribution of the assumed T_{wg} along the nozzle.

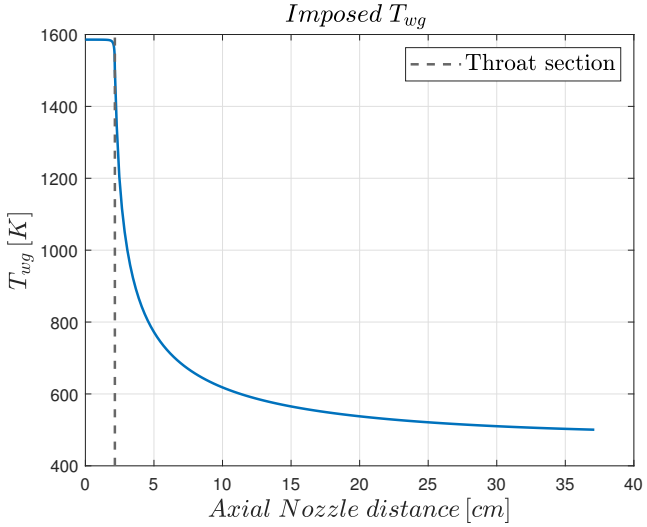

Figure 3: Assume distribution for the wall temperature at the gas side

The maximum allowed temperature for the wall side is at the inlet of the nozzle. The material selected is Nimonic Alloy 75, a nichel-chromium alloy with maximum allowed temperature of 1600K[8]. Hence, this value was set as the T_{wg} at the nozzle inlet. A more conservative approach should consider also lower values of the maximum reachable wall temperature to account for the decrease of material mechanical properties,
In this way, from the calculation of h_g also the heat flux along the nozzle can be evaluated, from the convergent to the exit section. The total heat rate can be estimated by integrating the heat flux over the internal area of the nozzle. This value can be found by numerical integration and the use of the Rao nozzle geometry introduced in **REFERENCE** . Finally, the increase of temperature of the fuel can be found by assuming the specific heat of the liquid.

$$\dot{Q} = \int_0^{L_{tot}} \dot{q} dx \tag{29}$$

$$\Delta T_{fu} = \frac{\dot{Q}}{c_{fu} \dot{m}_{fu}} \tag{30}$$

At this point, another consideration has to be pointed out: the condition that was set up by imposing the gas side wall temperature at its maximum (depending on the material choice) is a conservative choice since at the steady state it is related to the minimum flow that will be absorbed by the coolant (assuming fixed stationary gas flow conditions). If the coolant would not withstand this condition, the regenerative cooling could be excluded or eventually some other material or coating shall be used for the nozzle. Moreover, the blow-down architecture of the DRY-1 engine implies the reduction of the chamber pressure. This has major consequences on the heat transfer coefficient for the gas side. As a rule of thumb the h_g depends linearly on thrust chamber pressure, when this last value decrease the heat flux will also decrease (considering the same maximum wall temperature).
The heat transfer evaluation has also been combined with the system discharge dynamics (considering c^* as constant) in order to evaluate the heat flux rate, the heat rate and the increase of temperature for the fuel at every instant.

$\Delta T_{co,1}$ [K]	$\Delta T_{co,2}$ [K]	$\Delta T_{co,3}$ [K]
804.13	987.61	990.53

Table 7: Coolant increase of temperature considering three time instants

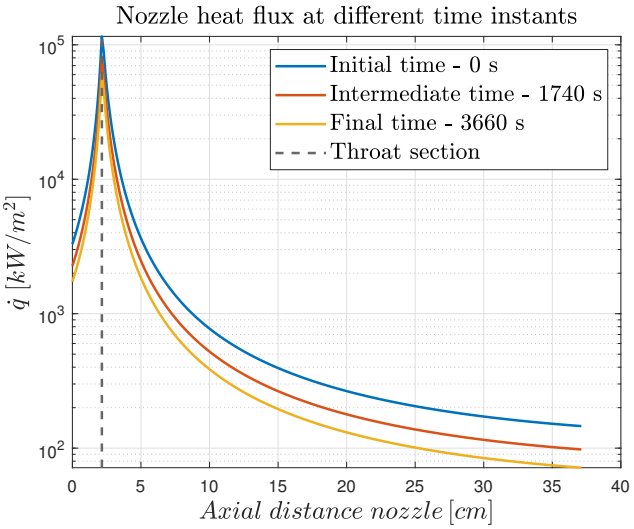

Figure 4: Heat flux along the nozzle at different time instants

From Table 7 it can be understood that the propellant mass flow rate of the fuel is not enough to absorb the heat without having several effects. Two opposite effect happens during the discharge of the blow-down: the decrease of the convective heat transfer coefficient related to the chamber pressure, but also the decrease of the propellant mass flow rate. The latter effect is prevailing since the increase of ΔT_{co} is larger at later time instants. Such high values of ΔT_{co} would bring to vaporize the fuel considering that the storing temperature of the RP-1 is 300 K (boiling temperature for RP-1 happens in the range 623K - 798K[9]). At high temperature decomposition process for the RP-1 can take place. Regarding the nozzle cooling, the radiative capability of the external wall shall be computed also considering other kinds of material or eventual internal coating.
Regarding the cooling of the thrust chamber, a viable option could be the introduction of a film cooling layer across the internal wall of the combustion chamber. The usage of hydrocarbon-based coolant with this technique revealed effective results. Under pressure of 130 bar, the hydrocarbons deposit acts as a thermal insulator hence

protecting the walls of the chamber[5]. In addition, the design of the film cooling should consider the re-design of the injector plate and should be evaluated in parallel with the material choice for the combustion chamber.

Bibliography

[1] Robert-Jan Koopmans et Al. “Propellant Tank Pressurisation with Helium Filled Hollow Glass Microspheres”. In: (2015).

[2] H. C. Hearn. “Design and Development of a Large Bipropellant Slowdown Propulsion System”. In: (1995).

[3] G.P.Sutton. “Rocket Propulsion Elements”. In: (2017).

[4] Ariane Group. *Chemical bipropellant thruster family*. Site: https://www.space-propulsion.com/. 2021.

[5] Huzel and Huang. “Modern Engineering for design of Liquid-Propellant Rocket Engines”. In: (1992).

[6] *NIST Chemistry WebBook*. URL: https://webbook.nist.gov/cgi/fluid.cgi?T=85&PLow=4&PHigh=5.5&PInc=0.1&Digits=5&ID=C7727379&Action=Load&Type=IsoTherm&TUnit=K&PUnit=bar&DUnit=mol%2Fl&HUnit=kJ%2Fkg&WUnit=m%2Fs&VisUnit=Pa*s&STUnit=N%2Fm&RefState=DEF. (accessed: 14.04.2024).

[7] Stephen D. Heister. “Rocket Propulsion”. In: (2019).

[8] Special Metals. *Nimonic Alloy 75*. Site: https://shorturl.at/ctzV7. 2004.

[9] Tim Edwards. “Liquid Fuels and Propellants for Aerospace Propulsion”. In: (2003).